

Molecular electronics and first-principles methods

J. J. Palacios,¹ A. J. Pérez-Jiménez,² E. Louis,^{1,3} J. A. Vergés,^{4,3} and E. SanFabián^{3,2}

¹*Departamento de Física Aplicada, Universidad de Alicante,
San Vicente del Raspeig, Alicante 03690, Spain.*

²*Departamento de Química-Física, Universidad de Alicante,
San Vicente del Raspeig, Alicante 03690, Spain.*

³*Unidad Asociada del Consejo Superior de Investigaciones Científicas,
Universidad de Alicante, San Vicente del Raspeig, Alicante 03690, Spain.*

⁴*Departamento de Teoría de la Materia Condensada,
Instituto de Ciencia de Materiales de Madrid (CSIC), Cantoblanco, Madrid 28049, Spain.*

We discuss the key steps that have to be followed to calculate coherent quantum transport in molecular and atomic-scale systems, making emphasis on the *ab-initio* Gaussian Embedded Cluster Method recently developed by the authors. We present various results on a simple system such as a clean Au nanocontact and the same nanocontact in the presence of hydrogen that illustrate the applicability of this method in the study and interpretation of a large range of experiments in the field of molecular electronics.

I. INTRODUCTION

Nanoscale electronics constitutes the backbone of present and future technological advances or, in other words, of Nanotechnology. Ultimately, the functionality of electronic devices will rely on the conduction properties of nanoscopic regions composed of a number of atoms that can range typically from several thousands down to a *single* one. Probably, the most promising research field within nanoscale electronics is what is known as molecular electronics. The main idea behind molecular electronics is the possibility that functional units can be built out of very stable and well-characterized molecules¹ such as fullerenes² or carbon nanotubes^{3,4}. The simplest molecular device consists of two large metallic electrodes, several nanometers apart, joined by a molecule or molecules anchored to them⁵. We will name this system molecular bridge. Alternatively, the electrodes can be simply connected by a chain of atoms of the same element as the electrodes^{6,7}. These bridges, generically known as atomic contacts or metallic nanocontacts, are not expected to be of any practical application, but constitute an excellent benchmark for us to learn about the world of electrical transport at the atomic scale.

The design and fabrication of electronic devices at the molecular and atomic scale poses new challenges for theorists who must develop and implement new techniques to address the upcoming problems. The basics to calculate the zero-bias, zero-temperature conductance G of a molecular bridge or metallic nanocontact were established by Landauer long before the concept of molecular electronics was commonplace. In Landauer's formalism G is simply related to the quantum mechanical transmission probability T of electrons at the Fermi level to go from one electrode to the other⁸ (we assume spin degeneracy):

$$G = G_0 T(E_F) = \frac{2e^2}{h} T(E_F). \quad (1)$$

The transmission can be easily estimated on generic con-

siderations for metallic nanocontacts^{9,10}, but it is much more difficult to do so for molecular bridges. The reason is simple: We do not know *a priori* where the electrode Fermi energy E_F lies with respect to the molecular levels. The positioning of E_F depends on two closely-related factors: (i) the coupling or hybridization of the molecular levels with the free-electron levels in the electrodes and (ii) the charge transfer between molecule and electrodes. The conductance is thus strongly dependent on the particular molecule, the detailed atomic arrangement of the electrodes where the molecule binds, and the chemical nature of the various elements at play. In order to give an answer to this problem we have to rely on first-principles or *ab-initio* calculations. To calculate the atomic arrangement of the electrodes or the way the molecule binds to the electrodes is a major problem in itself that deserves a whole study on its own and will not be given further consideration in these notes. Still, even if we ignore this important issue, to implement Landauer formalism requires to know the electronic structure of a finite region embedded in an infinite system with no particular symmetry or periodicity. This highly non-trivial problem is what we discuss in what follows.

II. THE BASICS

The main advantage of the numerical implementation that we discuss here with respect to similar proposals that have appeared in the literature^{11,12,13,14} is the use of a standard quantum chemistry code such as GAUSSIAN98¹⁵ (see Refs. 16,17,18,19). The GAUSSIAN98 code provides a versatile method to perform first-principles or *ab-initio* calculations of clusters, incorporating the major advancements in the field in terms of functionals, basis sets, pseudopotentials, etc.. The procedure goes as follows. A standard electronic structure calculation of the region that includes the molecule and a significant part of the electrodes is performed [see Fig. 1(a)]. This calculation can be performed within any mean-field-

like approach: Hartree-Fock or density functional (DF) theory in any of its multiple approximations. As far as transport is concerned, the self-consistent hamiltonian \hat{H} (or Fock matrix \hat{F}) of this central cluster or supermolecule contains the relevant information. The retarded(advanced) Green's functions associated with \hat{F}

$$\left[(E \pm i\delta) - \hat{F} \right] \hat{G}^{(\pm)} = \hat{I} \quad (2)$$

needs to incorporate the rest of the infinite electrodes:

$$\left[(E \pm i\delta) - \hat{F} - \hat{\Sigma}^{(\pm)} \right] \hat{G}^{(\pm)} = \hat{I} \quad (3)$$

In this expression

$$\hat{\Sigma}^{(\pm)} = \hat{\Sigma}_R^{(\pm)} + \hat{\Sigma}_L^{(\pm)}, \quad (4)$$

where $\hat{\Sigma}_R(\hat{\Sigma}_L)$ denotes a self-energy operator that accounts for the part of the right(left) semi-infinite electrode which has not been included in the calculation, and \hat{I} is the unity matrix. In a non-orthogonal basis the Green function takes the form

$$G_{NO}^{(\pm)} = S \left[(E \pm i\delta)S - F_{NO} - \Sigma_{NO}^{(\pm)} \right]^{-1} S \quad (5)$$

where S is the overlap matrix. To simplify the notation we have dropped the energy argument in the Green function and the selfenergy. The added self-energy matrices can only be explicitly calculated in ideal situations. We choose to describe the bulk electrode with a Bethe lattice tight-binding model with the coordination and parameters appropriate for the electrodes included in the cluster. Figure 1(c) depicts schematically a Bethe lattice of coordination three in two dimensions. The advantage of choosing a Bethe lattice resides in that it reproduces fairly well the bulk density of states of most commonly used metallic electrodes. For each atom in the outer planes of the cluster, we choose to add a branch of the Bethe lattice in the direction of any missing bulk atom (including those missing in the same plane). In Fig. 1(b) the directions in which Caylee tree branches are added are indicated by bigger atoms which represent the first atom of the branch in that direction. Assuming that the most important structural details of the electrode are included in the central cluster, the Bethe lattices should have no other relevance than that of introducing a generic reservoir.

The above definition of the Green function is not a standard one. As many other *ab-initio* implementations, GAUSSIAN98 makes use of non-orthogonal localized orbital basis sets. The appearance of S in the definition of the Green function guarantees that the total charge of the system N can be obtained through the standard expression used in quantum chemistry:

$$N = \text{Tr}[P \cdot S], \quad (6)$$

where the trace runs over all the atomic orbitals of the cluster and where P is the density matrix defined in a

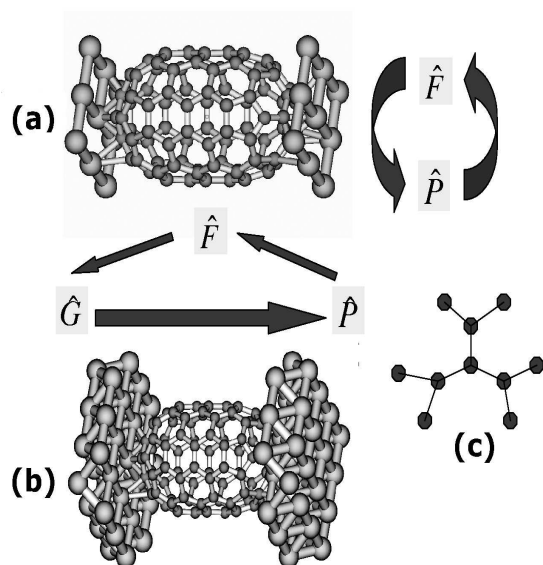


FIG. 1: (a) A molecular bridge model where a short capped nanotube is contacted by two (001) parallel surfaces. The standard self-consistent procedure performed initially by GAUSSIAN98 is also shown schematically on the right. (b) The same system where the first phantom atoms of the Bethe lattices are also depicted. The self-consistent procedure when the Bethe lattices are included is also shown schematically on top. (c) A finite section of a Bethe lattice model in two dimensions with coordination three.

standard way in terms of the retarded Green function as

$$P = -\frac{1}{\pi} \int_{-E_F}^{E_F} \text{Im} \left[S^{-1} G_{NO}^{(+)} S^{-1} \right] \quad (7)$$

E_F is the Fermi energy which can be set by imposing overall charge neutrality in the cluster. The integral in Eq. (7) can be efficiently calculated along a contour in the complex plane^{13,14,20}. As explained in the next section, we force GAUSSIAN98 to evaluate F using the density matrix defined in Eq. 7 instead of the standard one obtained from filling up the molecular orbitals obtained from diagonalizing the Fock matrix²¹. It is also interesting to note that the applicability of this approach, which we name the Gaussian Embedded Cluster Method (GECM) can be easily implemented in any quantum-chemistry or *ab-initio* code as long as it is based on a localized orbital expansion of the self-consistent, single-electron wavefunctions.

The transmission probability that appears in Eq. 1 can be calculated through the general expression⁸

$$T(E) = \text{Tr}[\hat{\Gamma}_L \hat{G}^{(+)} \hat{\Gamma}_R \hat{G}^{(-)}], \quad (8)$$

where Tr denotes the trace over all the orbitals of the cluster and where the operators $\hat{\Gamma}_{R(L)}$ are given by $i(\hat{\Sigma}_{R(L)} - \hat{\Sigma}_{R(L)}^\dagger)$. Finally, in order to single out the contribution of individual channels to the current, one can

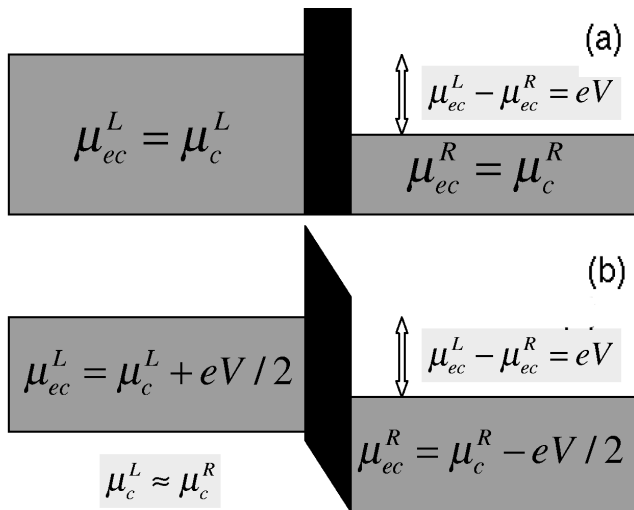


FIG. 2: Schematic picture of the development of a potential drop between electrodes separated by a barrier on imposing an electrochemical potential difference between them. (a) Before self-consistency begins the chemical potential in electrodes is different by an amount eV and the bottom of the conduction bands is the same for both electrodes. This situation corresponds to a diffusion problem. (b) After self-consistency has been achieved the chemical potential difference practically vanishes in favor of an electrostatic potential difference between electrodes.

diagonalize the transmission matrix. While the size of the matrix $[\hat{\Gamma}_L \hat{G}^{(-)} \hat{\Gamma}_R \hat{G}^{(+)}]$ can be as large as desired, the number of eigenvalues with a significant contribution will be typically much smaller, being determined by the narrowest part of the nanocontact or the molecule. The symmetry of each channel can be identified by looking at its weight on the atomic orbitals of the cluster.

Notice that, although the above expression provide us with the transmission as a function of energy, only the value of T at the Fermi energy, $T(E_F)$, is strictly correct (within the approximations inherent to DF theory). Away from E_F , $T(E)$ is only indicative. For instance, if a gate voltage is applied and the system gets charged or discharged, T needs to be recalculated for the new Fermi energy. To obtain the current I at non-zero temperature and finite bias voltage V one integrates the transmission probability:

$$I = \frac{2e}{h} \int_{-\infty}^{\infty} T(E, V) [f_L(E - eV/2) - f_R(E + eV/2)] dE, \quad (9)$$

where f_L and f_R are the Fermi distribution functions of the left and right electrodes, respectively. Notice, once again, that this innocent-looking expression is not a trivial generalization of Eq. 1 extended to finite bias voltages and temperature. The transmission coefficient that appears in the integrand $T(E, V)$ depends on temperature, but, most importantly, *depends on V* . To calculate this transmission coefficient, knowledge of the Fock matrix in

the presence of a bias voltage is required which, in turn, depends on the density matrix out of equilibrium. Based on standard non-equilibrium Green function techniques, it has been repeatedly shown in the literature⁸ that

$$P = -\frac{i}{2\pi} \int_{-\infty}^{\infty} dE [S^{-1} G^< S^{-1}] \quad (10)$$

where

$$\hat{G}^<(E) = i\hat{G}^{(-)}(E) \left[f_L(E) \hat{\Gamma}_L(E) + f_R(E) \hat{\Gamma}_R(E) \right] \hat{G}^{(+)}(E). \quad (11)$$

There are several technical and conceptual issues regarding the computation of the above equations that need some discussion. We refer the reader to the literature for a detailed account of most of them^{13,14,17}. Here we will simply mention two of them. Maybe the most important conceptual issue is that related to the fact that using DF theory for non-equilibrium situations is not justified: DF theory is a *ground-state* theory. We will make use of it simply because we do not know a better way to deal with out-of-equilibrium problems in an operative way. Second, there is technical issue that, in our view, has not received due attention in the literature and that we find it worth a detailed discussion²²: The out-of-equilibrium electrostatics. In most self-consistent approaches^{11,13,14,19} one solves the Poisson equation with boundary conditions appropriate for the electrode geometries. This is equivalent to imposing an external electric field and it can only be done for simple geometries such as infinite planes. The Keldysh formalism, however, does not necessarily require to deal with the Poisson equation if a significant part of the metallic electrodes has already been included in the central cluster. Thus, one can consider realistic electrode geometries if necessary. One simply imposes an *electrochemical potential* difference between electrodes $\mu_{ec}^L - \mu_{ec}^R = eV$ which is actually what a battery does. There are two contributions to μ_{ec} :

$$\mu_{ec} = \mu_{\text{chemical}} + \mu_{\text{electrostatic}}, \quad (12)$$

where we define

$$\begin{aligned} \mu_{\text{chemical}} &= \lim_{\delta N \rightarrow 0} \delta E_{\text{core}} / \delta N \\ \mu_{\text{electrostatic}} &= \lim_{\delta N \rightarrow 0} \delta E_{ee} / \delta N. \end{aligned}$$

E_{core} is the standard energy contribution to the total energy from the cores of the atoms and E_{ee} is the contribution from the electron-electron interaction³⁰. Specifically

$$\begin{aligned} \delta E_{\text{core}} &= \text{tr}[\delta P \cdot h_{\text{core}}] \\ \delta E_{ee} &= \text{tr}[\delta P \cdot h_{ee}], \end{aligned}$$

where h_{core} and h_{ee} are the core and interaction matrices composing the Fock matrix. In the selfconsistent procedure one electrode gets charged and the other discharged (by the same amount in case of mirror symmetry). Once self-consistency has been achieved, an electrostatic potential difference V between atoms one or

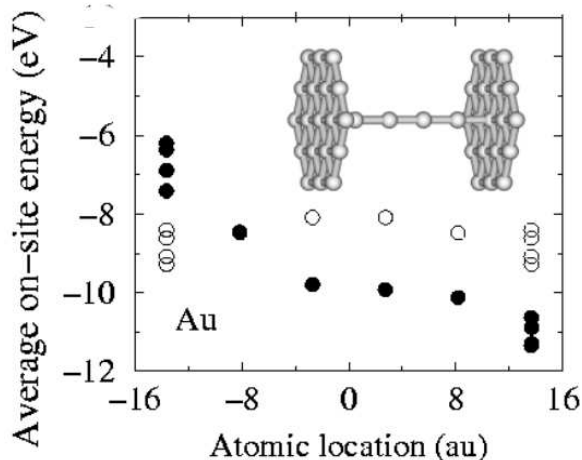


FIG. 3: Average on-site energies for all the atoms in the Au nanocontact shown in the inset. White dots have been obtained at zero bias and black dots at 5 V.

two layers inside opposite electrodes develops while their chemical potentials are similar, i.e., they remain neutral. On the other hand, the electrostatic potential drop will be smaller than V between atoms at the surface of opposite electrodes since they carry the charges. We show this process schematically in Fig. 2.

III. EXAMPLE: AU NANOCNTACTS

A. Clean nanocontacts

Calculations that illustrate the methodology described above have been carried out for the Au nanocontact shown in the inset of Fig. 3: Two (111) planes containing 19 atoms each plus a four-atom chain. Interatomic bulk distances have been taken for the whole cluster (2.88\AA), although one should keep in mind that an analysis of the structural stability of the nanocontact model is an important issue when one is interested in the interpretation of experimental data. The results shown next correspond to zero temperature and for the DF calculations we have used the Becke's three-parameter hybrid functional using the Lee, Yang and Parr correlation functional (B3LYP)²³ together with the semilocal shape consistent pseudopotential (SCPP) and minimal basis sets of Christiansen *et al.*^{24,25}. Fig. 3 shows the average on-site energies of the $5d6s6p$ orbitals for all the atoms of the nanocontact at zero and 5 V bias. This magnitude reflects the local self-consistent electrostatic potential on each atom. The results represented by white dots correspond to zero bias where one can see the characteristic potential profile due to the parallel surfaces reflected on the chain atoms lying across the vacuum between surfaces. The black dots correspond to a 5 V bias. One can see how an electrostatic potential drop of almost 5 V has developed between plates *without having imposed an external field, just an*

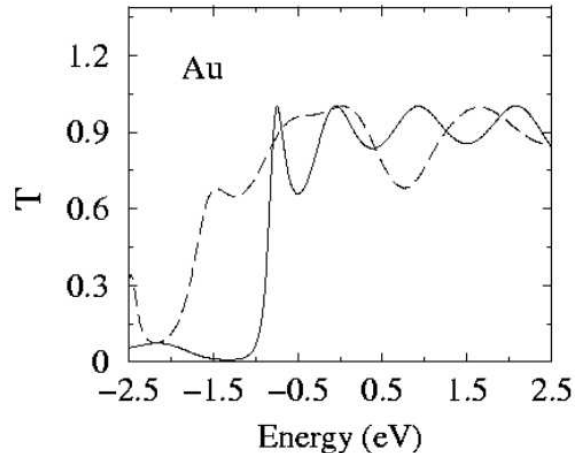


FIG. 4: Transmission versus energy for $V=0$ (continuous line) and 5 V (dashed line) for the Au nanocontact shown in Figure 3.

electrochemical potential difference. The major drop in the electrostatic potential occurs at the chain-plane contacts. In the case of zero bias the results are symmetric with respect to the geometric center of symmetry, as expected. Instead, a similar symmetry is absent for 5 V. Namely, whereas the potential drop between the left electrode and the first atom in the chain is 1.92 eV, it is only of 0.85 eV between the chain end and the right electrode. This feature seems common to all previously reported results^{13,26} and reflects bulk band structure features. The transmission T for zero and 5 V is shown in Fig.4. T oscillates around the Fermi energy with an upper limit value of one for both cases. This limit is well documented theoretical and experimentally for Au nanocontacts²⁷ since there is only one s -like channel around the Fermi energy for Au chains. The oscillations are due to scattering at the electrode-chain contact. This explains why conductance histograms exhibit the lowest peak slightly below $G = 2e^2/h$ ²⁸. It is worth noting that although the total current calculated by integrating $T(E, V = 0)$ in a window $[-V/2, V/2]$ does not differ much from that obtained with the full non-equilibrium approach, the differential conductance is significantly different. For instance, the gap below -0.5 eV is partially filled at finite bias.

B. H₂ molecular bridges in Au nanocontacts

We finally examine the possible consequences of adding hydrogen (H_2) to a Au nanocontact. A similar experimental analysis has been recently reported for Pt with conclusive results: The presence of H_2 molecules alters the conductance histograms of clean nanocontacts²⁹. It is thus important to determine the extent of this influence when interpreting conductance histograms under low-vacuum conditions or in the presence of gases. We considered here two electrodes in the form of pyramids

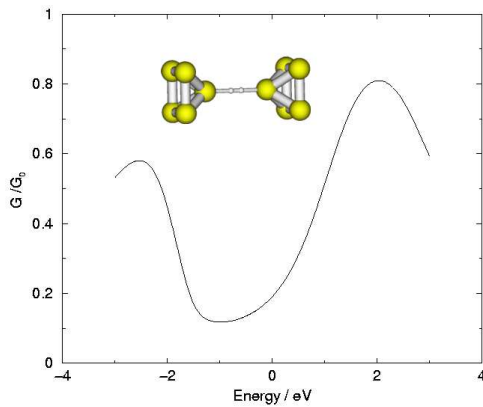


FIG. 5: Transmission versus energy for $V=0$ for the Au-H₂-Au bridge shown in the inset.

in the (001) direction with a H₂ molecule anchored between them (see inset in Fig. 5). The orientation of the molecule has been chosen on the basis of the report in Ref. 29 for Pt, although other alternatives have been recently proposed³¹. We have checked that this orientation is stable for a range of distances d between outer planes which are fixed in the relaxation. Finally we have computed the conductance for $d = 8 \text{ \AA}$ (shown in Fig. 5). As one can see the conductance at the Fermi energy is greatly reduced from the quantum of conductance G_0 due to the presence of the H₂ molecule. A detailed analysis of this problem will be published elsewhere³²

Financial support by the spanish MCYT (grants BQU2001-0883, PB96-0085, and MAT2002-04429-C03) and the Universidad de Alicante is gratefully acknowledged.

- ¹ C. Joachim, J. K. Gimzewski, and A. Aviram, *Nature* (London) **408**, 541 (2000).
- ² M. S. Dresselhaus, G. Dresselhaus, and P. C. Eklund, *Science of Fullerenes and Carbon Nanotubes* (Academic Press, San Diego, 1996).
- ³ R. Saito, G. Dresselhaus, and M. S. Dresselhaus, *Physical Properties of Carbon Nanotubes* (World Scientific, Singapore, 1998).
- ⁴ C. Dekker, *Physics Today* **52**, 22 (1999).
- ⁵ M. A. Reed, C. Zhou, C. J. Muller, T. P. Burgin, and J. M. Tour, *Science* **278**, 252 (1997).
- ⁶ C. J. Muller, J. M. van Ruitenbeek, and L. J. de Jong, *Phys. Rev. Lett.* **69**, 140 (1992).
- ⁷ N. Agrait, J. C. Rodrigo, and S. Vieira, *Phys. Rev. B* **47**, 12345 (1993).
- ⁸ S. Datta, *Electronic transport in mesoscopic systems* (Cambridge University Press, Cambridge, 1995).
- ⁹ J. C. Cuevas, A. Levy-Yeyati, and A. Martín-Rodero, *Phys. Rev. Lett.* **80**, 1066 (1998).
- ¹⁰ A. Hasmy, E. Medina, and P. A. Serena, *Phys. Rev. Lett.* **86**, 5574 (2001).
- ¹¹ N. D. Lang, *Phys. Rev. B* **52**, 5335 (1995).
- ¹² K. Hirose and M. Tsukada, *Phys. Rev. B* **51**, 5278 (1995).
- ¹³ M. Brandbyge, J. L. Mozos, P. Ordejón, J. Taylor, and K. Stokbro, *Phys. Rev. B* **65**, 165401 (2002).
- ¹⁴ J. Taylor, H. Guo, and J. Wang, *Phys. Rev. B* **63**, 245407 (2001).
- ¹⁵ M. J. Frisch, G. W. Trucks, H. B. Schlegel, M. A. R. G. E. Scuseria, J. R. Cheeseman, V. G. Zakrzewski, J. A. Montgomery, Jr., R. E. Stratmann, J. C. Burant, et al., *GAUSSIAN98*, Revision A.7, Gaussian, Inc., Pittsburgh PA, 1998.
- ¹⁶ J. J. Palacios, A. J. Pérez-Jiménez, E. Louis, and J. A. Vergés, *Phys. Rev. B* **64**, 115411 (2001).
- ¹⁷ J. J. Palacios, A. J. Pérez-Jiménez, E. Louis, E. SanFabián, and J. A. Vergés, *Phys. Rev. B* **66**, 035322 (2002).
- ¹⁸ J. J. Palacios, A. J. Pérez-Jiménez, E. Louis, and J. A. Vergés, *Nanotechnology* **12**, 160 (2001).
- ¹⁹ P. S. Damle, A. W. Ghosh, and S. Datta, *Phys. Rev. B* **64**, 201403 (2001).
- ²⁰ Y. Xue, S. Datta, and M. A. Ratner, arXiv:cond-mat/0112136.
- ²¹ A. Szabo and N. S. Ostlund, *Modern Quantum Chemistry* (McGraw-Hill, New York, 1989).
- ²² E. Louis, J. A. Vergés, J. J. Palacios, A. J. Pérez-Jiménez, and E. SanFabián, arXiv:cond-mat/0212115.
- ²³ A. D. Becke, *J. Chem. Phys.* **98**, 5648 (1993).
- ²⁴ L. F. Pacios and P. A. Christiansen, *J. Chem. Phys.* **82**, 2664 (1985).
- ²⁵ M. M. Hurley, L. F. Pacios, P. A. Christiansen, R. B. Ross, and W. C. Ermler, *J. Chem. Phys.* **84**, 6840 (1986).
- ²⁶ M. Brandbyge, N. Kobayashi, and N. Tsukada, *Phys. Rev. B* **60**, 17064 (1999).
- ²⁷ N. Agrait, A. Levi-Yeyati, and J. van Ruitenbeek, to be published.
- ²⁸ L. G. C. Rego, A. R. Rocha, V. Rodrigues, and D. Ugarte, arXiv:cond-mat/0206412.
- ²⁹ R. H. M. Smit, Y. Noat, C. Untiedt, N. D. Lang, M. C. van Hemert, and J. M. van Ruitenbeek, *Nature* (London) **419**, 906 (2002).
- ³⁰ Note that this definition is not a standard one in the sense that one usually thinks of external fields when referring to the electrostatic potential contribution to the electrochemical potential. Instead we will make use of this term when referring to any contribution coming from electron-electron interactions. Strictly speaking, however, one should not use the term electrostatic potential since there are exchange and correlation contributions included in DF theory.
- ³¹ Y. García, J. J. Palacios, E. Louis, J. A. Vergés, E. SanFabián, and A. J. Pérez-Jiménez, unpublished.
- ³² Y. Garcia, J. J. Palacios, A. J. P'erez-Jiménez, E. Louis, E. SanFabián, and J. A. Vergés, unpublished.